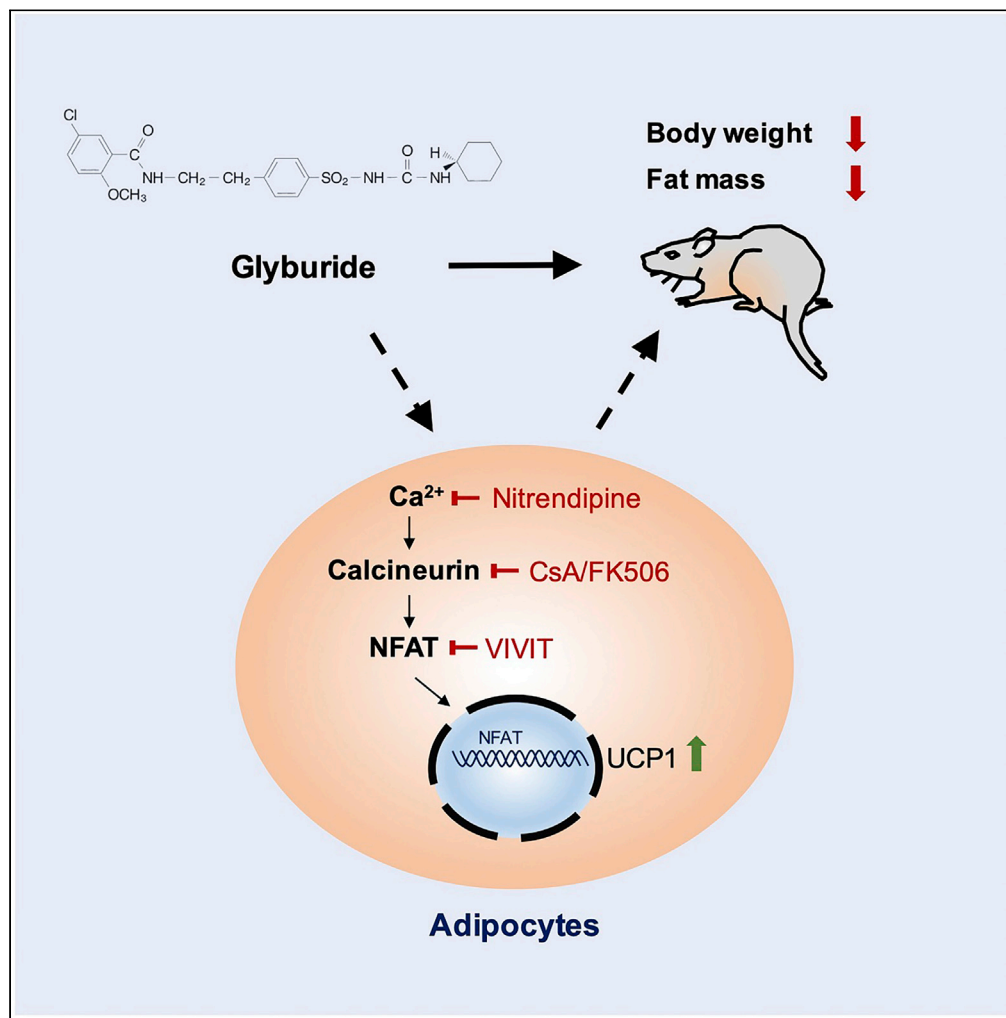


Article

Glyburide Regulates UCP1 Expression in Adipocytes Independent of K_{ATP} Channel Blockade

Yan Qiu, Yuanyuan Yang, Yuda Wei, ..., Lanlan Chen, Lijun Luo, Qirong Ding

qrding@sibs.ac.cn

HIGHLIGHTS

Glyburide significantly upregulated UCP1 expression in both brown and white adipocytes

Glyburide-fed mice exhibited a clear resistance to high-fat diet-induced obesity

The glyburide effect in UCP1 expression in adipocytes was K_{ATP} independent

Glyburide effect in UCP1 level was reversed by the Calcineurin-NFAT pathway inhibition

Article

Glyburide Regulates UCP1 Expression in Adipocytes Independent of K_{ATP} Channel Blockade

Yan Qiu,¹ Yuanyuan Yang,¹ Yuda Wei,¹ Xiaojian Liu,¹ Zhuanghui Feng,¹ Xuwen Zeng,² Yanhao Chen,¹ Yan Liu,¹ Yongxu Zhao,¹ Lanlan Chen,¹ Lijun Luo,² and Qiurong Ding^{1,3,4,*}

SUMMARY

Identification of safe and effective compounds to increase or activate UCP1 expression in brown or white adipocytes remains a potent therapeutic strategy to combat obesity. Here we reported that, glyburide, one of the FDA-approved drugs currently used to treat type 2 diabetes, can significantly enhance UCP1 expression in both brown and white adipocytes. Glyburide-fed mice exhibited a clear resistance to high-fat diet-induced obesity, reduced blood triglyceride level, and increased UCP1 expression in brown adipose tissue. Moreover, *in situ* injection of glyburide to inguinal white adipose tissue remarkably enhanced UCP1 expression and increased thermogenesis. Further mechanistic studies indicated that the glyburide effect in UCP1 expression in adipocytes was K_{ATP} channel independent but may involve the regulation of the Ca^{2+} -Calcineurin-NFAT signal pathway. Overall, our findings revealed the significant effects of glyburide in regulating UCP1 expression and thermogenesis in adipocytes, which can be potentially repurposed to treat obesity.

INTRODUCTION

Obesity is becoming a global pandemic as a result of sustained energy intake exceeding energy expenditure under a modern lifestyle. The discovery that the brown and beige adipose tissues can burn energy to heat instead of energy storing highlights pharmacological activation of brown adipose tissue or induction of beige adipose tissue as promising strategies to target obesity (Inagaki et al., 2016; Harms and Seale, 2013; Betz and Enerback, 2018). The energy burning properties of brown or beige adipocytes lies mostly in the expression of UCP1 (uncoupling protein 1), a protein that is highly expressed in brown and beige adipocytes and localized on the inner mitochondrial membrane. When activated, UCP1 uncouples oxidative respiration from ATP synthesis, resulting in heat generation (Fedorenko et al., 2012). Therefore, UCP1 serves as a promising molecular target to thermogenesis enhancement and obesity treatment. Although plenty of compounds have been reported to increase UCP1 expression in adipocytes (Andrade et al., 2014; Van Dam et al., 2015; Zhang et al., 2014; Lu et al., 2016; Feng et al., 2019), safe and effective compounds that can be used clinically are still lacking.

We have previously developed a cellular screening platform with the *Ucp1*-2A-GFP reporter cell lines, which allows high-throughput screenings using a fluorescence signal as readout (Qiu et al., 2018). Using this reporter line, we have identified a group of drugs that can upregulate UCP1 expression in brown adipocytes and reported suturent as an effective modulator of UCP1 expression in brown adipose tissue (Qiu et al., 2018). Suturent belongs to the tyrosine kinase (RTK) inhibitor family and has been used clinically to treat certain kidney, pancreatic, and gastrointestinal cancers. Although suturent treatment did not cause obvious adverse effect in our study in animals, side effects observed in patients renders it impossible for immediate repurposing to treat obesity.

It is very interesting that Glyburide, one of the drugs used in lowering blood glucose, has shown a strong effect in upregulating UCP1 in brown adipocytes in our screening. Glyburide is a sulfonylurea drug, also known as glibenclamide in Europe, which can directly bind to and block the SUR1 subunits of ATP-dependent potassium channels (K_{ATP}) and consequently increase insulin secretion from the pancreatic β cells. Glyburide has been approved to treat type 2 diabetes clinically (Malek and Davis, 2016), which has also been repurposed for the treatment of acute central nervous system injury recently (King et al., 2018).

¹CAS Key Laboratory of Nutrition, Metabolism and Food Safety, Shanghai Institute of Nutrition and Health, Shanghai Institutes for Biological Sciences, University of Chinese Academy of Sciences, Chinese Academy of Sciences, Shanghai 200031, P. R. China

²The Affiliated Stomatology Hospital of Tongji University, 399 Yanchang Road, Shanghai 200072, P. R. China

³Institute for Stem Cell and Regeneration, Chinese Academy of Sciences, Beijing 100101, P. R. China

⁴Lead Contact

*Correspondence:

qrding@sibs.ac.cn

<https://doi.org/10.1016/j.isci.2020.101446>



Previous studies have indicated an interesting aspect of ions channels and the electrophysiological modulation in the regulation of thermogenesis activity in brown and beige adipocytes. For example, KCNK3, a two-pore-domain potassium channel, which promotes outward K^+ current and limits Ca^{2+} influx, has been shown to affect thermogenesis in brown and beige adipocytes. KCNK3 is highly expressed in brown and beige adipose and is directly regulated by PRDM16. KCNK3 impairs thermogenesis via antagonizing NE-induced membrane depolarization and Ca^{2+} influx to decrease cAMP production (Chen et al., 2017; Pisani et al., 2016). TRPV2, a Ca^{2+} -permeable non-selective cation channel, was also reported to play vital roles in brown adipose tissue (Sun et al., 2016). Lack of TRPV2 impaired thermogenesis in mouse brown adipose tissue. It is still unclear how TRPV2 activation modulates thermogenesis; however, the induction of thermogenic genes in response to β 3-adrenergic receptor stimulation was decreased in TRPV2KO brown adipocytes and suppressed by reduced intracellular Ca^{2+} concentrations in wild-type brown adipocytes.

Combining the previous strong indication of glyburide in upregulating UCP1 in brown adipocytes and the interest whether the effect of glyburide is through K_{ATP} channel inhibiting, we decided to focus on the functional study of glyburide in adipocytes and to explore the underlying mechanism.

RESULTS

Glyburide Enhanced UCP1 Expression in Adipocytes *In Vitro*

Our previous screening suggested strong upregulating effect of glyburide in UCP1 expression in brown adipocytes. We first validated the effect of glyburide in *in vitro* cultured brown adipocytes. Initially, mature brown adipocytes were treated with 10 μ M glyburide at day 8 after the maintenance stage for 1 day (Figure 1A). The lipid content was not changed after glyburide treatment, indicating glyburide had no effect on adipocyte differentiation (Figure 1B). Consistent with the high-throughput screening results, glyburide treatment significantly increased UCP1 expression in brown adipocytes, at both the mRNA level and the protein level, compared with cells treated with DMSO (Figures 1C and 1D). Glyburide treatment also stimulated expression of other thermogenic or brown differentiation genes, including *Cidea*, *Pgc1a*, *Ppara*, and *Prdm16* (Figure 1D). To know whether the glyburide effect is dependent on treatment time point, we then treated cells with glyburide for 3 days at the maintenance stage or 8 days along the whole differentiation process (Figures S1A and S1F). Under these two conditions, cells treated with glyburide both displayed increased UCP1 expression (Figures S1B–S1D and S1G–S1I) and enhanced expression of other thermogenic or brown differentiation genes (Figures S1C and S1H), although with no significant difference as compared with 1-day treatment at day 8 (Figures 1C and 1D) and with no significant change on adipocyte differentiation either (Figures S1E and S1J). Additionally, UCP1 expression was also significantly increased in day 8 brown adipocytes after glyburide treatment for as short as 4 h, indicating that glyburide stimulates UCP1 expression in a very short time in mature brown adipocytes (Figures S1K and S1L).

We next tested the effect of glyburide in cultured white adipocytes. Mature white adipocytes were treated with glyburide for 4 days (Figure 1F), and the lipid accumulation was not changed after glyburide treatment (Figure 1G). We noticed significant increase in UCP1 expression upon glyburide treatment at both the mRNA and protein levels (Figures 1H and 1I). We also observed increased expression of other thermogenic genes, including *Cidea* and *Pgc1a*, indicating the induction of a browning process in white adipocytes (Figure 1I). Moreover, glyburide effect was also tested after treatment in the whole white adipocyte differentiation process. Cells were treated with glyburide for 8 days during the whole differentiation process for 8 days (Figure S2A). Results demonstrated that glyburide treatment significantly improved UCP1 expression (Figures S2B–S2D), and with a stronger UCP1 induction effect after longer time treatment (Figure S2D), with no significant change on adipocyte differentiation (Figure S2E).

To get a better understanding of glyburide effect, we next performed RNA sequencing (RNA-seq) for glyburide or DMSO-treated brown and white adipocytes. Gene ontology (GO) analysis revealed that glyburide treatment in brown adipocytes led to significant upregulation of in total 505 genes using a cutoff of $p \leq 0.05$, which were enriched for lipid metabolic process, fat cell differentiation, and thermogenesis (Figure 1E). A total of 404 genes were upregulated in white adipocytes after glyburide treatment, which were also significantly enriched in lipid metabolic process, brown fat differentiation, oxidation reduction process, and others (Figure 1J). Among these upregulated genes, 100 genes were common genes regulated in both brown and white adipocytes after glyburide treatment (Figure 1K), including important regulators in lipid metabolism, such as *Fgf21*, *Elovl3*, *Ppara*, and *Scd3* (Figure 1L). Altogether, these data demonstrated that glyburide treatment promoted UCP1 and thermogenesis gene expression in both brown and white adipocytes.

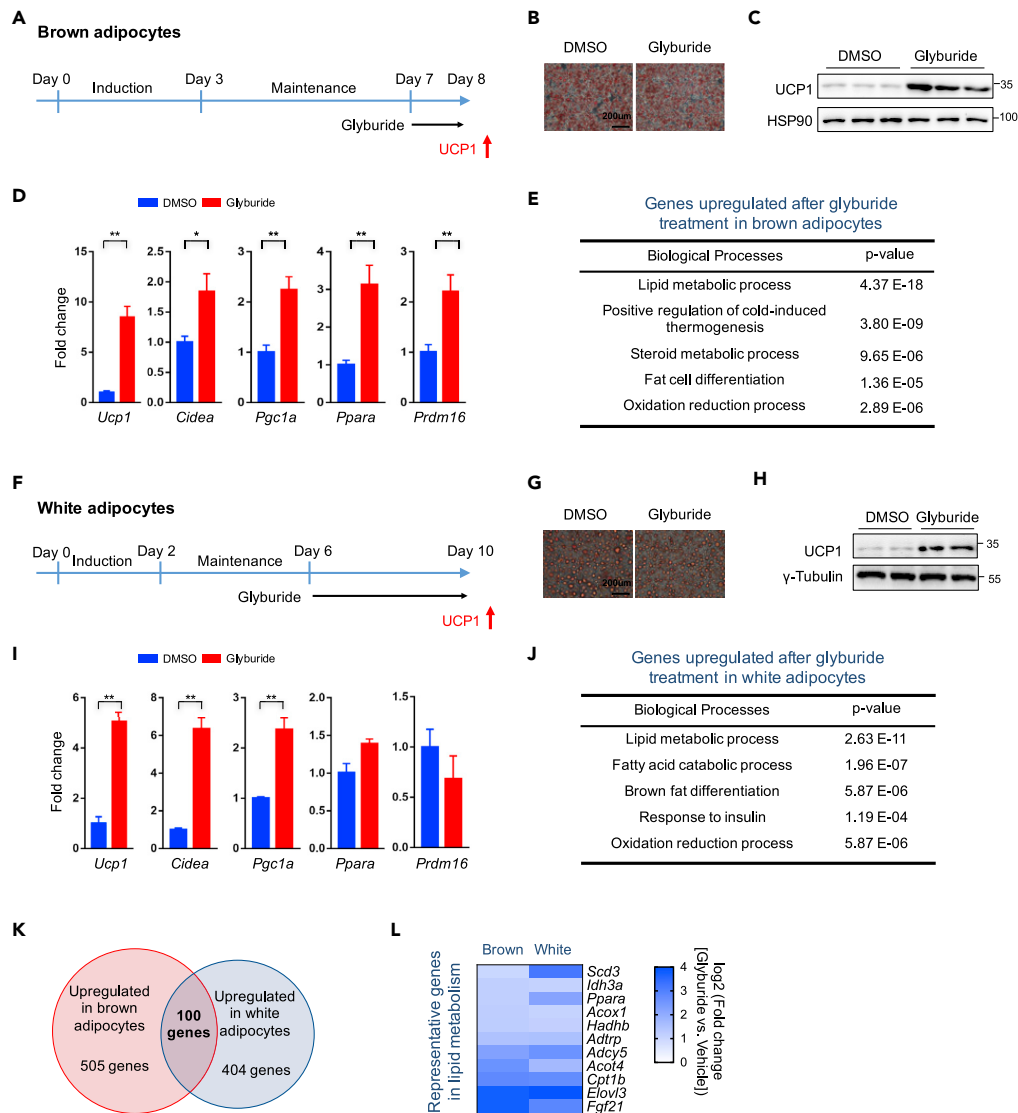


Figure 1. Glyburide Promoted UCP1 Expression in Both Brown and White Adipocytes

(A) Schematic view of the brown adipocyte differentiation procedure and compound treatment protocol. Cells were treated with 10 μ M glyburide or DMSO for 1 day after 7 days' differentiation and collected at day 8 for analysis. (B) Assessment of lipid accumulation (evaluated by Oil Red O staining) in glyburide or DMSO-treated *Ucp1*-2A-GFP brown adipocytes. Scale bar, 200 μ m. (C) Western blot analysis of UCP1 protein expression in glyburide or DMSO-treated *Ucp1*-2A-GFP brown adipocytes. (D) mRNA expression analyses of genes in glyburide or DMSO-treated *Ucp1*-2A-GFP brown adipocytes. $n = 4$. (E) Gene Ontology analyses of regulated genes in brown adipocytes after glyburide treatment identified by RNA-seq. (F) Schematic view of the white adipocyte differentiation procedure and compound treatment protocol. Cells were treated with 10 μ M glyburide or DMSO for 4 days after 6 days' differentiation and collected at day 10 for analysis. (G) Assessment of lipid accumulation (evaluated by Oil Red O staining) in glyburide or DMSO-treated *Ucp1*-2A-GFP white adipocytes. Scale bar, 200 μ m. (H) Western blot analysis of UCP1 protein expression in glyburide or DMSO-treated *Ucp1*-2A-GFP white adipocytes. (I) mRNA expression analyses of genes in glyburide or DMSO-treated *Ucp1*-2A-GFP white adipocytes. $n = 3$. (J) Gene Ontology analyses of regulated genes in white adipocytes after glyburide treatment identified by RNA-seq. (K) Venn analysis of upregulated genes from brown and white adipocytes after glyburide treatment. (L) Heatmap depicting upregulated genes related to lipid metabolism in brown and white adipocytes after glyburide treatment.

Bars show mean \pm SEM. p Values are shown for indicated comparisons by the Student's t test. * $p < 0.05$, ** $p < 0.01$. See also Figures S1 and S2.

Glyburide Enhanced UCP1 Expression in Adipose Tissues *In Vivo*

We next investigated the effect of glyburide treatment *in vivo*. Mice were fed with high-fat diet (HFD) and treated with glyburide at the dose of 2 mg/kg/day through oral administration for 11 week (Figure 2A). Glyburide treatment caused significant body weight loss (−9% after 11-week treatment) (Figure 2B), whereas no significant change was observed in food intake (Figure S3A). Serum analyses showed a clear reduction of total triglyceride (TG) (−35.92%), with no significant change of total cholesterol (TC) or free fatty acid contents in mice treated with glyburide (Figures 2C and S3B). Consistent with body weight loss, organ weights of BAT (brown adipose tissue, −9.76%), eWAT (epididymal white adipose tissue, −32.97%), and iWAT (inguinal white adipose tissue, −30.6%) were reduced significantly in glyburide-treated mice (Figure 2D). The reduction in body and organ weights were mostly caused by decrease in fat mass (−29.52%) as revealed by the NMR analysis (Figure 2E). Furthermore, histological analyses of adipose tissues displayed significantly reduced adipocyte size in BAT, eWAT, and iWAT (Figure 2F), although no significant change was observed in liver triglyceride or liver cholesterol content (Figure S3C). Consistent with the results in cultured cells, glyburide treatment resulted in significant increase of UCP1 expression in brown adipose tissue (Figure 2G). Metabolic analysis displayed a minor increase in O₂ consumption after glyburide treatment, if calculated with normalization to body weight (Figures 2H and 2I); however, no significant change in net O₂ consumption was observed (Figures S3G and S3H). In the meantime, there was minimal change in physical activity (Figure S3D). Besides, expression levels of other thermogenic genes, including *Cidea*, *Dio2*, *Pgc1a*, *Ppara*, and *Prdm16*, in brown adipose tissue were not changed after glyburide treatment (Figures S3E and S3F). Altogether, these results indicated that the phenotypic changes observed in mice after glyburide treatment are at least partly caused by improved UCP1 expression in brown adipose tissue.

We also treated mice with a lower dose of 50 μg/kg/day via oral administration, which is more relevant to the therapeutic glyburide doses used clinically (Remedi and Nichols, 2008). Low-dose glyburide treatment did not cause significant change in either body weight or body composition in mice under HFD (Figures S4A and S4C). Besides, low-dose glyburide treatment led to no significant change in energy expenditure, as reflected by minimal change of O₂ consumption and CO₂ content, with the comparable physical activity (Figures S4E and S4G). Food intake monitoring did not show significant change after glyburide treatment (Figure S4B). Serum analysis indicated no significant change in total cholesterol or in total triglyceride level in mice treated with glyburide under HFD (Figure S4D). Mice were then dissected for further investigation. Overall, there was no significant change in total organ weight or adipocytes sizes in BAT, eWAT, or iWAT (Figures S4F and S4H). We then tested the insulin and blood glucose responses of animals to different doses of glyburide via oral administration. We found that 2 mg/kg glyburide caused a marked increase of insulin release and rapid drop of blood glucose level, whereas 50 μg/kg glyburide had no effect on the insulin and blood glucose contents of mice (Figures S4I and S4J), suggesting different drug sensitivity of glyburide between human beings and mice.

We suspected that the reason we did not observe a significant phenotypic change in animals after low-dose treatment of glyburide is because the drug cannot reach the adipose tissues, especially when delivered via oral administration. We thus next tested the effect of glyburide directly through *in situ* injection to inguinal white adipose depot. CL-316243 injection was used as a positive control. Four days after a single injection, mice were dissected and inguinal adipose tissues were obtained for UCP1 expression analysis (Figure 3A). Similar to CL-316243 treatment, we observed a remarkable increase in UCP1 expression in inguinal white adipose depot after glyburide treatment (Figure 3B). HE and UCP1 staining also displayed a clear browning phenomenon in inguinal adipose tissue, as indicated by smaller lipid droplets and enhanced UCP1 expression (Figure 3C). In consistency with increased UCP1 expression, levels of the OXPHOS proteins were also increased in glyburide-treated white adipose tissues (Figure 3D). Moreover, glyburide-treated mice displayed higher rectal temperature in the cold challenge experiment (Figure 3E). These results altogether demonstrated that glyburide treatment promoted white adipose browning *in vivo*.

The Effect of Glyburide in UCP1 Upregulation Was K_{ATP} Independent

Glyburide is a second-generation sulfonylurea drug that has been used to treat patients with type 2 diabetes mellitus. It stimulates insulin secretion through the closure of ATP-sensitive potassium channels (K_{ATP}) on pancreatic β cells, raising intracellular calcium ion concentration (Gribble and Reimann, 2003). The K_{ATP} channel is a heterooctameric complex composed of four inwardly rectifying pore-forming K⁺ channel subunits (Kir6.x; Kir6.1 or Kir6.2) and four regulatory sulfonylurea receptor SUR ATP-binding cassettes subunits (SUR; SUR1 or SUR2) (Nichols, 2006). Diverse classes of K_{ATP} channels exist, which differ from each other in different tissues and cell types in terms of their nucleotide sensitivities, their biophysical properties,

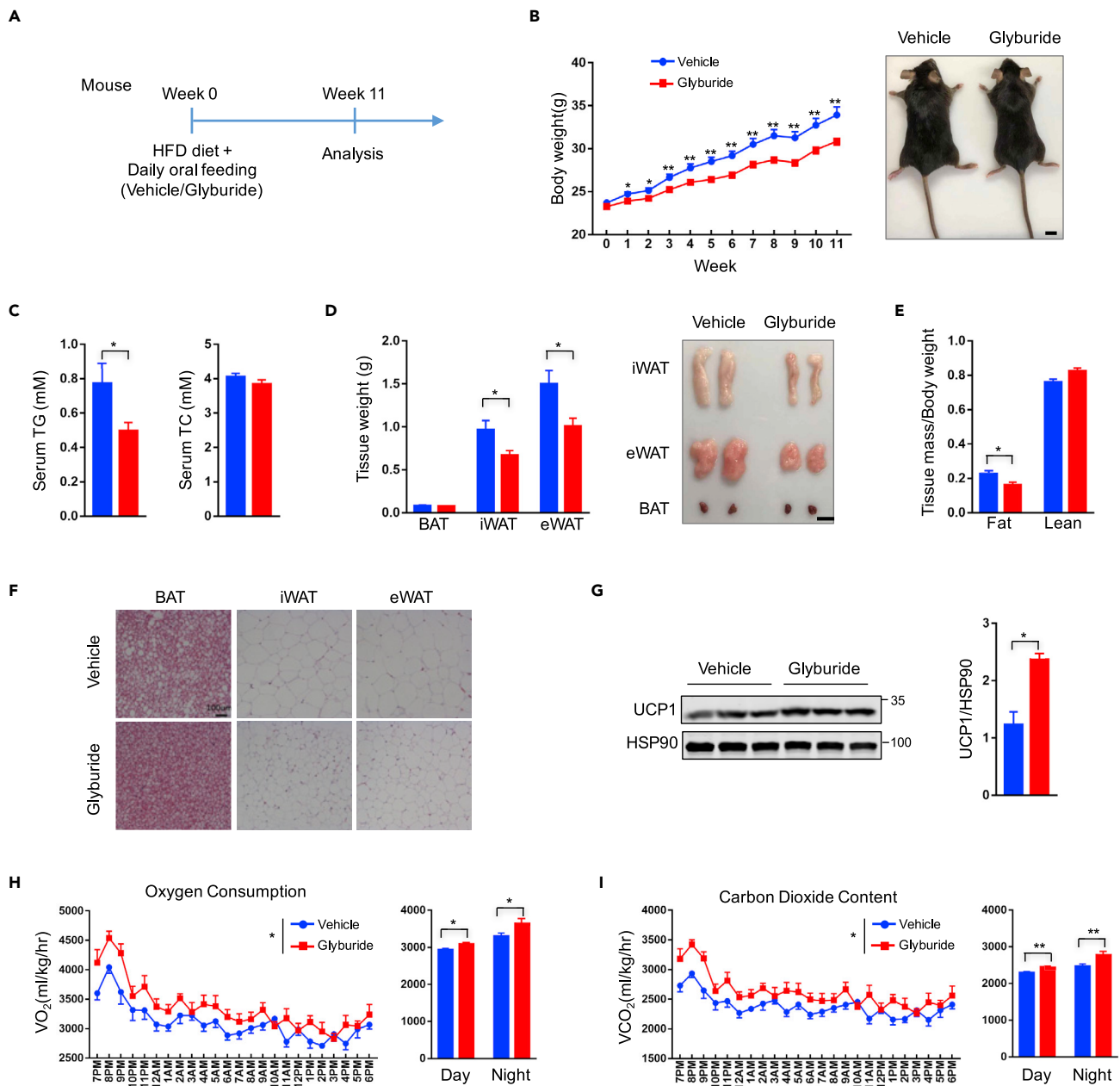


Figure 2. Glyburide Treatment Promoted Weight Loss of Mice under HFD

(A) Schematic view of mouse experiments. Mice were administrated 2 mg/kg glyburide or vehicle through daily oral feeding under HFD for 11 weeks.

(B) Body weights of mice treated with glyburide or vehicle under HFD (left) and representative image of mouse treated with glyburide or vehicle 11 weeks later (right). $n = 12$. Scale bar, 1 cm.

(C) Serum total triglyceride (TG) and total cholesterol (TC) content of mice measured after 11-week treatment with glyburide or vehicle. $n = 12$.

(D) Weights of different mouse adipose tissues (left) and representative fat images of different mouse adipose tissues (right) after 11-week treatment with glyburide or vehicle. $n = 12$. Scale bar, 1 cm.

(E) Body lean and fat composition of mice determined by NMR after 10-week treatment with glyburide or vehicle. $n = 12$.

(F) Representative HE staining images of BAT, iWAT, and eWAT. Scale bar, 100 μ m.

(G) Western blot analysis of UCP1 protein expression level in mouse brown adipose tissues.

(H) Oxygen consumption measurement of mice in metabolic cages after 11-week treatment with glyburide or vehicle. $n = 8$.

(I) CO₂ content measurement of mice in metabolic cages after 11-week treatment with glyburide or vehicle. $n = 8$.

Bars show mean \pm SEM. p Values are shown for indicated comparisons by the Student's t test (B–E and G) or two-way ANOVA (H and I). * $p < 0.05$, ** $p < 0.01$. See also Figures S3 and S4.

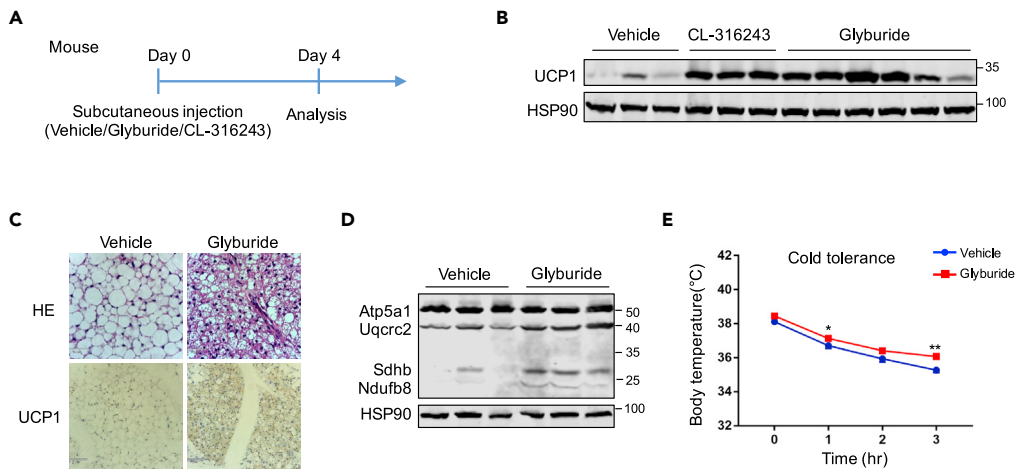


Figure 3. Glyburide Treatment Improved UCP1 Expression in Inguinal White Adipose Tissue

(A) Schematic view of mouse experiments. Mice were administrated 1 mg/kg glyburide, 1 mg/kg CL-316243, or vehicle through subcutaneous injection. Four days after a single injection, mice were dissected and inguinal white adipose tissues were obtained for further analysis.

(B) UCP1 protein expression analyses of inguinal white adipose tissue after compound treatment with as indicated.

(C) Representative images of H&E staining and UCP1 staining of inguinal white adipose tissue after glyburide or vehicle treatment. Scale bar, 210 μ m.

(D) OXPHOS protein expression analyses in inguinal white adipose tissue of mice treated with glyburide or vehicle.

(E) Cold challenge experiment with vehicle or glyburide-treated mice. n = 8. Bars show mean \pm SEM. p Values are shown for indicated comparisons by the Student's t test. *p < 0.05, **p < 0.01.

and their sensitivities to pharmacological agents (Foster and Coetzee, 2016). In pancreatic β cells Kir6.2/SUR1 are the major subunits expressed, in cardiac myocytes Kir6.2/SUR2A subunits, in smooth muscles SUR2B, whereas in adipose tissue Kir6.1/SUR2B are the major forms (Szeto et al., 2018). To directly assess whether K_{ATP} channel is involved in UCP1 upregulation by glyburide, we next knocked out either Kir subunits or SUR subunits of K_{ATP} channels using the CRISPR-Cas technology in adipocytes. We screened individual sgRNAs targeting *Kir6.1*, *Kir6.2*, *Sur1*, as well as *Sur2* genes. All sgRNAs demonstrated high editing activity in brown adipocytes (Figure 4A). However, we did not observe significant change of UCP1 expression either at the mRNA level or the protein level after depleting two *Kir* genes (*Kir*-sgRNAs: *Kir6.1*-sgRNA and *Kir6.2*-sgRNA) or two *Sur* genes (*Sur*-sgRNAs: *Sur1*-sgRNA and *Sur2*-sgRNA) in brown adipocytes. In the meantime, glyburide treatment still upregulated UCP1 expression in *Kir*-sgRNAs and *Sur*-sgRNAs cells, showing no significant difference in comparison with the effect in control cells (Figures 4B–4D). These results demonstrated that, although glyburide was supposed to target K_{ATP} channel, it stimulated the expression of UCP1 in adipocytes in a K_{ATP} channel-independent manner. Moreover, Epac2, which is a guanine nucleotide exchange factor for the small guanosine triphosphatase Rap1, was reported to be another direct target of antidiabetic sulfonylurea drugs (Zhang et al., 2009). We therefore next tested whether glyburide increases UCP1 expression via targeting Epac2. We screened an sgRNA targeting the second exon of the mouse *Epac2* gene, which showed high editing activity (Figure S5A). However, we did not observe significant increase of UCP1 expression in *Epac2*-KO brown adipocytes, and meanwhile, *Epac2*-KO did not abrogate the effect of glyburide in upregulating UCP1 expression (Figures S5B, S5C, and S5F).

To further confirm whether the glyburide effect in UCP1 upregulation is K_{ATP} independent or Epac2 independent, we chose another four compounds that can also target K_{ATP} or/and Epac2 (Figure 4E). However, only glyburide treatment was able to increase UCP1 expression in brown adipocytes, with little effect from other compounds (Figures 4F and 4G). Furthermore, treatment with a combination of four compounds had no effect in UCP1 expression or the UCP1 upregulation by glyburide (Figure 4H). Similarly, only glyburide, but none of the other four K_{ATP} inhibitors, was able to increase UCP1 expression in white adipocytes (Figure 4I). Taken together, these results suggest a unique feature of glyburide that upregulates UCP1 expression, which is K_{ATP} independent and Epac2 independent.

Caveolin was previously reported to be involved in the action of glimepiride, a sulfonylurea drug with very close structure with glyburide. Caveolin was tyrosine phosphorylated in isolated rat adipocytes in response to

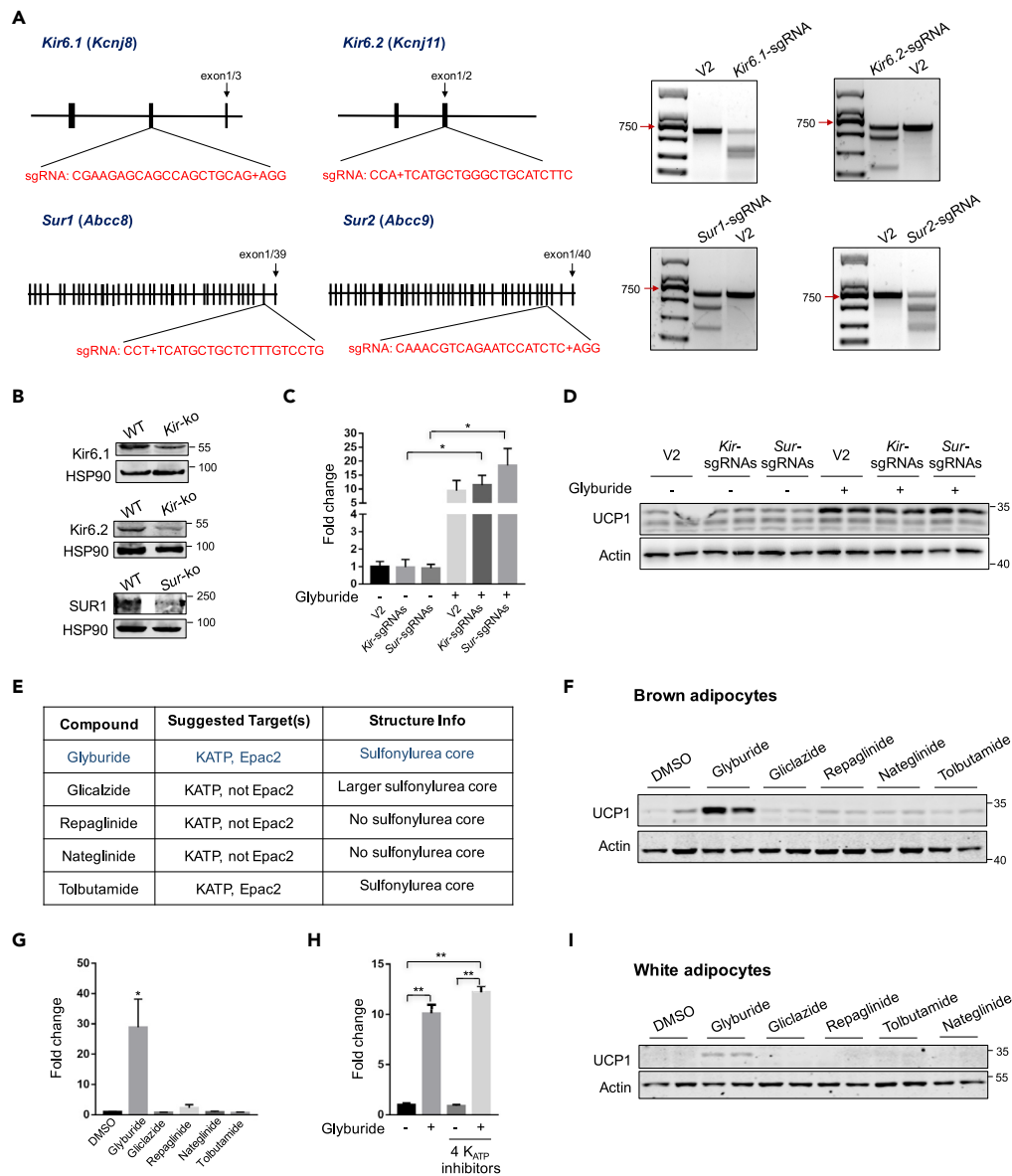


Figure 4. Glyburide Increased UCP1 Expression Independent of KATP Blockade

(A) Schematic view of CRISPR sgRNAs design for indicated genes and genome editing activity of selected sgRNAs was indicated.

(B) Western blot analyses of indicated proteins in CRISPR sgRNAs-treated brown adipocytes.

(C) *Ucp1* mRNA expression analyses of brown adipocytes treated with CRISPRs and compounds as indicated. $n = 3$.

(D) UCP1 protein expression analyses of brown adipocytes treated with CRISPRs and compounds as indicated.

(E) The suggested target(s) and structure information of selected compounds.

(F) UCP1 protein expression analyses of brown adipocytes treated with compounds (10 μ M) as indicated.

(G) *Ucp1* mRNA expression analyses of brown adipocytes treated with compounds (10 μ M) as indicated. $n = 3$.

(H) *Ucp1* mRNA expression analyses of brown adipocytes treated with compounds as indicated. $n = 3$.

(I) UCP1 protein expression analyses of white adipocytes treated with compounds as indicated.

Bars show mean \pm SEM. p Values are shown for indicated comparisons by the Student's t test. * $p < 0.05$, ** $p < 0.01$. See also Figure S5.

glimepiride treatment, playing important functions in transmembrane signal transduction (Muller, 2000; Muller et al., 2005). Moreover, caveolin-1 (Cav1) is expressed abundantly in adipose tissue and involved in many physiological processes. 3T3-L1 adipocytes overexpressing Cav1 were better differentiated (Chang et al., 2017). We

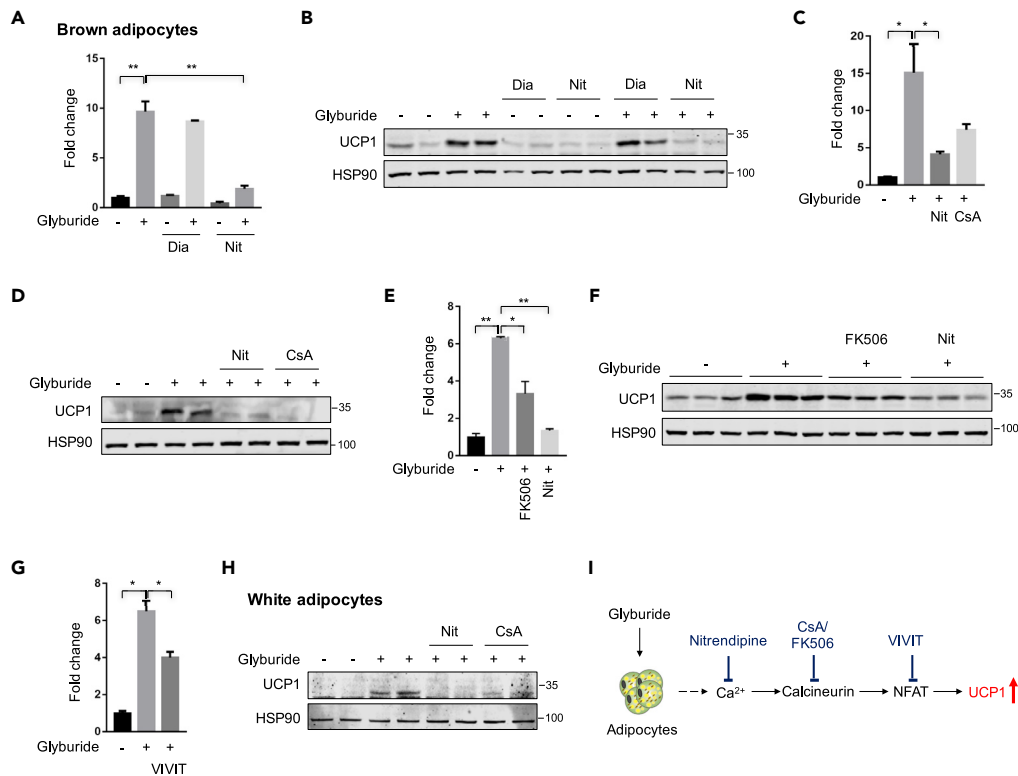


Figure 5. Glyburide's Effect in UCP1 Upregulation Was Blocked by the Inhibition of Ca^{2+} -Calcineurin-NFAT Signal Pathway

(A) *Ucp1* mRNA expression analyses of brown adipocytes treated with compounds as indicated. n = 3.
 (B) UCP1 protein expression analyses of brown adipocytes treated with compounds as indicated.
 (C) *Ucp1* mRNA expression analyses of brown adipocytes treated with compounds as indicated. n = 3.
 (D) UCP1 protein expression analyses of brown adipocytes treated with compounds as indicated.
 (E) *Ucp1* mRNA expression analyses of brown adipocytes treated with compounds as indicated. n = 3.
 (F) UCP1 protein expression analyses of brown adipocytes treated with compounds as indicated.
 (G) *Ucp1* mRNA expression analyses of brown adipocytes treated with compounds as indicated. n = 3.
 (H) UCP1 protein expression analyses of white adipocytes treated with compounds as indicated.
 (I) The schematic diagram of a working mechanism that glyburide regulates UCP1 expression in adipocytes. Compounds used for treatment were as following: 10 μ M Glyburide, 10 μ M Diazoxide (Dia), 30 μ M Nitrendipine (Nit), 10 μ M Cyclosporine A (CsA), 10 μ M FK506 (Calcineurin inhibitor), 10 μ M VIVIT (NFAT inhibitor). Bars show mean \pm SEM. p Values are shown for indicated comparisons by the Student's t test. *p < 0.05, **p < 0.01.

thus next wanted to know whether the effect of glyburide is regulated through Cav1. We also targeted the mouse *Cav1* gene using the CRISPR technology (Figure S5D). However, we did not observe significant change in UCP1 expression in *Cav1*-KO brown adipocytes with or without glyburide treatment (Figures S5E and S5F).

The Effect of Glyburide in UCP1 Upregulation Was Reversed by the Inhibition of the Ca^{2+} -Calcineurin-NFAT Signal Pathway

Glyburide can increase cytosolic Ca^{2+} levels in isolated rat adipocytes in a concentrated manner, which was blocked by nitrendipine, an L-type Ca^{2+} channel antagonist (Draznin et al., 1987, 1988). We thus treated the cells with nitrendipine to test whether the glyburide effect in UCP1 expression was mediated by the increase in intracellular Ca^{2+} levels. We also tested cells with another compound, diazoxide, a potassium channel activator, which was also reported to counteract the effect of glyburide in adipocytes (Shi et al., 1999). Results showed that nitrendipine (Nit) significantly blocked the UCP1 expression induced by glyburide treatment. However, diazoxide (Dia) did not cause significant change in UCP1 expression under basal level or upon glyburide treatment (Figures 5A and 5B), further confirming that the glyburide effect in UCP1 upregulating is not dependent on potassium channels but may involve regulation from intracellular Ca^{2+} levels. Transient receptor potential vanilloid 2 (TRPV2), a Ca^{2+} -permeable non-selective cation channel,

was reported to have critical roles in thermogenesis in mouse brown adipose tissue (Sun et al., 2016). We next tested whether the glyburide effect in UCP1 expression was regulated by the TRPV2 channel. We targeted the mouse *Trpv2* gene using the CRISPR technology (Figure S5G). However, we did not observe significant change of UCP1 expression in *Trpv2*-KO brown adipocytes, with or without glyburide treatment (Figures S5H and S5I), suggesting that the glyburide upregulated UCP1 was not through TRPV2.

We next further tested whether glyburide upregulated UCP1 via the Ca^{2+} -Calcineurin-NFAT signaling (Crabtree and Schreiber, 2009) by adding the calcineurin inhibitor, cyclosporine A (CsA) or FK506, to glyburide-treated brown adipocytes. Results showed that, similar to nitrendipine, both CsA and FK506 treatment effectively blocked the glyburide effect in UCP1 elevation (Figures 5C–5F). Moreover, the NFAT inhibitor, VIVIT, which is a cell-permeable peptide inhibitor of nuclear factor of activated T cells (NFAT) that selectively inhibits calcineurin-mediated dephosphorylation of NFAT (Ma et al., 2019), also significantly affected the increase of *Ucp1* expression induced by glyburide treatment (Figure 5G). Similarly, in white adipocytes, the UCP1 upregulation upon glyburide treatment was also blocked by calcineurin inhibition (Figure 5H). Altogether, these data suggested that the glyburide effect in UCP1 upregulation could be reversed by the inhibition of Ca^{2+} -Calcineurin-NFAT signal pathway (Figure 5I).

DISCUSSION

Taken together, our study has identified that glyburide, a drug used in clinical treatment of type 2 diabetes, can effectively promote UCP1 expression in brown and white adipocytes, both *in vitro* and *in vivo*. The mechanism of UCP1 upregulation, however, is not mediated by inhibition of the K_{ATP} channel, a well-known target of glyburide. Although the direct target(s) of glyburide in upregulating UCP1 in adipocytes is still unknown, our results suggested the involvement of the Ca^{2+} -Calcineurin-NFAT signal pathway in the underlying mechanism.

In our *in vivo* investigations, we found that, when treated with a high dose, glyburide can significantly decrease the gain of whole-body weight due to HFD feeding, and reduce blood triglyceride levels, at least partly due to improved UCP1 expression in brown adipose tissue. However, decreased body weight and blood lipids have not been observed in clinical patients taking glyburide. We suspect that the reason is mainly because the rather low efficiency of glyburide reaching adipose tissues by oral administration. This is similar to animal experiments treated with a low dose of glyburide, in which no obvious phenotypic change was observed. High dose of glyburide will certainly cause severe and life-threatening side effect as low blood glucose; it is therefore unacceptable to increase the dose in patients for the achievement of weight loss effect. As our results demonstrated that *in situ* injection of glyburide directly to the white adipose depots in animals had a strong effect in UCP1 upregulation and thermogenesis enhancement, different approaches for local adipose tissue delivering, for example, local delivery through a microneedle patch (Zhang et al., 2017), is essentially the way to go.

The effect of glyburide in adipocytes is not limited to the increase of UCP1 expression, but glyburide imposes a broad effect to the expression of many genes involved in lipid metabolism and thermogenesis, as revealed by the RNA-seq analyses. It is impressive that glyburide treatment led to a significant increase in *Fgf21* expression in both brown and white adipocytes. FGF21 is a protein with multiple metabolic protective reactions, and indeed a bright star on the metabolic disease therapeutic horizon. In fact, several clinical trials are ongoing focusing on FGF21 therapy to metabolic diseases (Sanyal et al., 2019; Gaich et al., 2013; Kim et al., 2017). Our discovery that glyburide can boost the expression of *Fgf21* in adipocytes revealed another beneficial aspect of glyburide treatment, besides the UCP1 upregulation and its long-term safety *in vivo*. However, in a different aspect, to what extent the upregulation of UCP1 explains in the whole phenotypic change upon glyburide treatment would need further investigation, ideally with the *Ucp1* knockout animals.

The direct target(s) of glyburide in adipocyte is intriguing and remains undefined. Glyburide is known to stimulate insulin secretion through closure of the K_{ATP} channel in the pancreatic β cells; however, our results suggest that the K_{ATP} channel is not its target in adipocytes in regulating UCP1 expression. The direct comparison results of glyburide with other K_{ATP} targeting compounds also confirmed the conclusion and suggested different target(s) responsible for the effect of glyburide in UCP1 regulation. Our initial tests with several inhibitors suggest that the Ca^{2+} -Calcineurin-NFAT signaling pathway may involve in the effect of glyburide. The Ca^{2+} -Calcineurin-NFAT signaling pathway can transmit signals to the nucleus from a wide variety of receptors and is important to developmental events such as axon outgrowth, cardiac morphogenesis, and immune responses (Crabtree and Schreiber, 2009). Previous evidence indicated that the Regulator of Calcineurin 1 (*RCAN1*), a feedback inhibitor of the calcium-activated protein

phosphatase calcineurin, was a negative regulator of UCP1 expression in white adipose tissue. Mice lacking *Rcan1* were resistant to diet-induced obesity (Rotter et al., 2018). Besides, several reports also pointed out the possible important regulating function of NFAT in adipocyte biology. For example, mice deficient for *Nfatc2* and *Nfatc4* were protected from diet-induced obesity (Yang et al., 2006). And in human, polymorphisms for *NFATc4* gene may confer certain protection or predisposition for the development of new-onset diabetes after kidney allograft transplantation (Chen et al., 2012). Also, genome-wide association studies (GWASs) indicated that the *NFATc1*, *NFATc2*, and *NFATc4* loci are associated with a variety of metabolic traits (Ramos et al., 2014). However, to what extent the glyburide effects in adipocytes depend on the Ca^{2+} -Calcineurin-NFAT signaling pathway is worth further investigation. Despite these unknowns, the findings that glyburide can increase UCP1 expression in adipocytes both *in vitro* and *in vivo* may shed light on new treatment of obesity and related metabolic diseases.

Limitations of the Study

In the present study, we showed that glyburide effect in UCP1 upregulation was K_{ATP} independent but may involve the regulation of Ca^{2+} -Calcineurin-NFAT signaling pathway. However, further investigations are required to characterize the detailed mechanisms. Additionally, *Ucp1* knockout mice will be helpful to establish the physiological relevance of UCP1 upregulation with the phenotypic change upon glyburide treatment in animals.

Resource Availability

Lead Contact

Further information and requests for resources should be directed to and will be fulfilled by the Lead Contact, Qirong Ding (qrding@sibs.ac.cn).

Materials Availability

All unique materials generated from this study are available from the Lead Contact with a complete Materials Transfer Agreement.

Data and Code Availability

Raw data were deposited in NCBI Sequence Read Archive (SRA) with the accession number: PRJNA645978.

METHODS

All methods can be found in the accompanying [Transparent Methods supplemental file](#).

SUPPLEMENTAL INFORMATION

Supplemental Information can be found online at <https://doi.org/10.1016/j.isci.2020.101446>.

ACKNOWLEDGMENTS

This work was supported by grants from the National Key R&D Program of China (2017YFA0102800, 2017YFA0103700), the Strategic Priority Research Program of the Chinese Academy of Sciences (XDA16030402), and the National Natural Science Foundation of China (31670829, 31971063).

AUTHOR CONTRIBUTIONS

Y.Q. and Q.D. conceived and designed research studies, analyzed the data, prepared figures, and wrote the manuscript. Y.Q. performed all the experiments. Y.Y., Y.W., X.L., Z.F., X.Z., Y.C., and L.C. assisted with the mouse studies. Y.L., Y.Z., and L.L. provided advice. Q.D. supervised the project.

DECLARATION OF INTERESTS

The authors declare no competing interests.

Received: April 23, 2020

Revised: July 8, 2020

Accepted: August 6, 2020

Published: September 25, 2020

REFERENCES

- Andrade, J.M., Frade, A.C., Guimaraes, J.B., Freitas, K.M., Lopes, M.T., Guimaraes, A.L., De Paula, A.M., Coimbra, C.C., and Santos, S.H. (2014). Resveratrol increases brown adipose tissue thermogenesis markers by increasing SIRT1 and energy expenditure and decreasing fat accumulation in adipose tissue of mice fed a standard diet. *Eur. J. Nutr.* 53, 1503–1510.
- Betz, M.J., and Enerback, S. (2018). Targeting thermogenesis in brown fat and muscle to treat obesity and metabolic disease. *Nat. Rev. Endocrinol.* 14, 77–87.
- Chang, C.C., Chen, C.Y., Wen, H.C., Huang, C.Y., Hung, M.S., Lu, H.C., Chen, W.L., and Chang, C.H. (2017). Caveolin-1 secreted from adipose tissues and adipocytes functions as an adipogenesis enhancer. *Obesity (Silver Spring)* 25, 1932–1940.
- Chen, Y., Sampaio, M.S., Yang, J.W., Min, D., and Hutchinson, I.V. (2012). Genetic polymorphisms of the transcription factor NFATc4 and development of new-onset diabetes after transplantation in Hispanic kidney transplant recipients. *Transplantation* 93, 325–330.
- Chen, Y., Zeng, X., Huang, X., Serag, S., Woolf, C.J., and Spiegelman, B.M. (2017). Crosstalk between KCNK3-mediated ion current and adrenergic signaling regulates adipose thermogenesis and obesity. *Cell* 171, 836–848.e13.
- Crabtree, G.R., and Schreiber, S.L. (2009). SnapShot: Ca²⁺-calcineurin-NFAT signaling. *Cell* 138, 210–210.e1.
- Draznin, B., Kao, M., and Sussman, K.E. (1987). Insulin and glyburide increase cytosolic free-Ca²⁺ concentration in isolated rat adipocytes. *Diabetes* 36, 174–178.
- Draznin, B., Sussman, K.E., Eckel, R.H., Kao, M., Yost, T., and Sherman, N.A. (1988). Possible role of cytosolic free calcium concentrations in mediating insulin resistance of obesity and hyperinsulinemia. *J. Clin. Invest.* 82, 1848–1852.
- Fedorenko, A., Lishko, P.V., and Kirichok, Y. (2012). Mechanism of fatty-acid-dependent UCP1 uncoupling in brown fat mitochondria. *Cell* 151, 400–413.
- Feng, Z., Wei, Y., Zhang, Y., Qiu, Y., Liu, X., Su, L., Liang, N., Yin, H., and Ding, Q. (2019). Identification of a rhodanine derivative BML-260 as a potent stimulator of UCP1 expression. *Theranostics* 9, 3501–3514.
- Foster, M.N., and Coetzee, W.A. (2016). KATP channels in the cardiovascular system. *Physiol. Rev.* 96, 177–252.
- Gaich, G., Chien, J.Y., Fu, H., Glass, L.C., Deeg, M.A., Holland, W.L., Kharitonov, A., Bumol, T., Schilske, H.K., and Moller, D.E. (2013). The effects of LY2405319, an FGF21 analog, in obese human subjects with type 2 diabetes. *Cell Metab.* 18, 333–340.
- Gribble, F.M., and Reimann, F. (2003). Sulphonylurea action revisited: the post-cloning era. *Diabetologia* 46, 875–891.
- Harms, M., and Seale, P. (2013). Brown and beige fat: development, function and therapeutic potential. *Nat. Med.* 19, 1252–1263.
- Inagaki, T., Sakai, J., and Kajimura, S. (2016). Transcriptional and epigenetic control of brown and beige adipose cell fate and function. *Nat. Rev. Mol. Cell Biol.* 17, 480–495.
- Kim, A.M., Somayaji, V.R., Dong, J.Q., Rolph, T.P., Weng, Y., Chabot, J.R., Gropp, K.E., Talukdar, S., and Calle, R.A. (2017). Once-weekly administration of a long-acting fibroblast growth factor 21 analogue modulates lipids, bone turnover markers, blood pressure and body weight differently in obese people with hypertriglyceridaemia and in non-human primates. *Diabetes Obes. Metab.* 19, 1762–1772.
- King, Z.A., Sheth, K.N., Kimberly, W.T., and Simard, J.M. (2018). Profile of intravenous glyburide for the prevention of cerebral edema following large hemispheric infarction: evidence to date. *Drug Des. Devel. Ther.* 12, 2539–2552.
- Lu, P., Zhang, F.C., Qian, S.W., Li, X., Cui, Z.M., Dang, Y.J., and Tang, Q.Q. (2016). Artemisinin derivatives prevent obesity by inducing browning of WAT and enhancing BAT function. *Cell Res.* 26, 1169–1172.
- Ma, J.D., Jing, J., Wang, J.W., Mo, Y.Q., Li, Q.H., Lin, J.Z., Chen, L.F., Shao, L., Miossec, P., and Dai, L. (2019). Activation of the peroxisome proliferator-activated receptor gamma coactivator 1beta/NFATc1 pathway in circulating osteoclast precursors associated with bone destruction in rheumatoid arthritis. *Arthritis Rheumatol.* 71, 1252–1264.
- Malek, R., and Davis, S.N. (2016). Pharmacokinetics, efficacy and safety of glyburide for treatment of gestational diabetes mellitus. *Expert Opin. Drug Metab. Toxicol.* 12, 691–699.
- Muller, G. (2000). The molecular mechanism of the insulin-mimetic/sensitizing activity of the antidiabetic sulfonylurea drug Amaryl. *Mol. Med.* 6, 907–933.
- Muller, G., Schulz, A., Wied, S., and Frick, W. (2005). Regulation of lipid raft proteins by glimepiride- and insulin-induced glycosylphosphatidylinositol-specific phospholipase C in rat adipocytes. *Biochem. Pharmacol.* 69, 761–780.
- Nichols, C.G. (2006). KATP channels as molecular sensors of cellular metabolism. *Nature* 440, 470–476.
- Pisani, D.F., Beranger, G.E., Corinus, A., Giroud, M., Ghandour, R.A., Altiriba, J., Chambard, J.C., Mazure, N.M., Bendahou, S., Duranton, C., et al. (2016). The K⁺ channel TASK1 modulates beta-adrenergic response in brown adipose tissue through the mineralocorticoid receptor pathway. *FASEB J.* 30, 909–922.
- Qiu, Y., Sun, Y., Xu, D., Yang, Y., Liu, X., Wei, Y., Chen, Y., Feng, Z., Li, S., Reyad-ul Ferdous, M., et al. (2018). Screening of FDA-approved drugs identifies suture as a modulator of UCP1 expression in brown adipose tissue. *EBioMedicine* 37, 344–355.
- Ramos, E.M., Hoffman, D., Junkins, H.A., Maglott, D., Phan, L., Sherry, S.T., Feolo, M., and Hindorf, L.A. (2014). Phenotype-Genotype Integrator (PheGenI): synthesizing genome-wide association study (GWAS) data with existing genomic resources. *Eur. J. Hum. Genet.* 22, 144–147.
- Remedi, M.S., and Nichols, C.G. (2008). Chronic antidiabetic sulfonylureas in vivo: reversible effects on mouse pancreatic beta-cells. *PLoS Med.* 5, e206.
- Rotter, D., Peiris, H., Grinsfelder, D.B., Martin, A.M., Burchfield, J., Parra, V., Hull, C., Morales, C.R., Jessup, C.F., Matusica, D., et al. (2018). Regulator of Calcineurin 1 helps coordinate whole-body metabolism and thermogenesis. *EMBO Rep.* 19, e44706.
- Sanyal, A., Charles, E.D., Neuschwander-Tetri, B.A., Loomba, R., Harrison, S.A., Abdelmalek, M.F., Lawitz, E.J., Hulegoua-Demazio, D., Kundu, S., Noviello, S., et al. (2019). Pegbelfermin (BMS-986036), a PEGylated fibroblast growth factor 21 analogue, in patients with non-alcoholic steatohepatitis: a randomised, double-blind, placebo-controlled, phase 2a trial. *Lancet* 392, 2705–2717.
- Shi, H., Moustaid-Moussa, N., Wilkison, W.O., and Zemel, M.B. (1999). Role of the sulfonylurea receptor in regulating human adipocyte metabolism. *FASEB J.* 13, 1833–1838.
- Sun, W., Uchida, K., Suzuki, Y., Zhou, Y., Kim, M., Takayama, Y., Takahashi, N., Goto, T., Wakabayashi, S., Kawada, T., et al. (2016). Lack of TRPV2 impairs thermogenesis in mouse brown adipose tissue. *EMBO Rep.* 17, 383–399.
- Szeto, V., Chen, N.H., Sun, H.S., and Feng, Z.P. (2018). The role of KATP channels in cerebral ischemic stroke and diabetes. *Acta Pharmacol. Sin.* 39, 683–694.
- Van Dam, A.D., Nahon, K.J., Kooijman, S., Van Den Berg, S.M., Kanhai, A.A., Kikuchi, T., Heemskerk, M.M., Van Harmelen, V., Lombes, M., Van Den Hoek, A.M., et al. (2015). Salsalate activates brown adipose tissue in mice. *Diabetes* 64, 1544–1554.
- Yang, T.T., Suk, H.Y., Yang, X., Olabisi, O., Yu, R.Y., Durand, J., Jelicks, L.A., Kim, J.Y., Scherer, P.E., Wang, Y., et al. (2006). Role of transcription factor NFAT in glucose and insulin homeostasis. *Mol. Cell Biol.* 26, 7372–7387.
- Zhang, C.L., Katoh, M., Shibasaki, T., Minami, K., Sunaga, Y., Takahashi, H., Yokoi, N., Iwasaki, M., Miki, T., and Seino, S. (2009). The cAMP sensor Epac2 is a direct target of antidiabetic sulfonylurea drugs. *Science* 325, 607–610.
- Zhang, Y., Liu, Q., Yu, J., Yu, S., Wang, J., Qiang, L., and Gu, Z. (2017). Locally induced adipose tissue browning by microneedle patch for obesity treatment. *ACS Nano* 11, 9223–9230.
- Zhang, Z., Zhang, H., Li, B., Meng, X., Wang, J., Zhang, Y., Yao, S., Ma, Q., Jin, L., Yang, J., et al. (2014). Berberine activates thermogenesis in white and brown adipose tissue. *Nat. Commun.* 5, 5493.

iScience, Volume 23

Supplemental Information

Glyburide Regulates UCP1 Expression in Adipocytes Independent of K_{ATP} Channel Blockade

Yan Qiu, Yuanyuan Yang, Yuda Wei, Xiaojian Liu, Zhuanghui Feng, Xuwen Zeng, Yanhao Chen, Yan Liu, Yongxu Zhao, Lanlan Chen, Lijun Luo, and Qirong Ding

Supplemental Information

Supplemental figures and legends

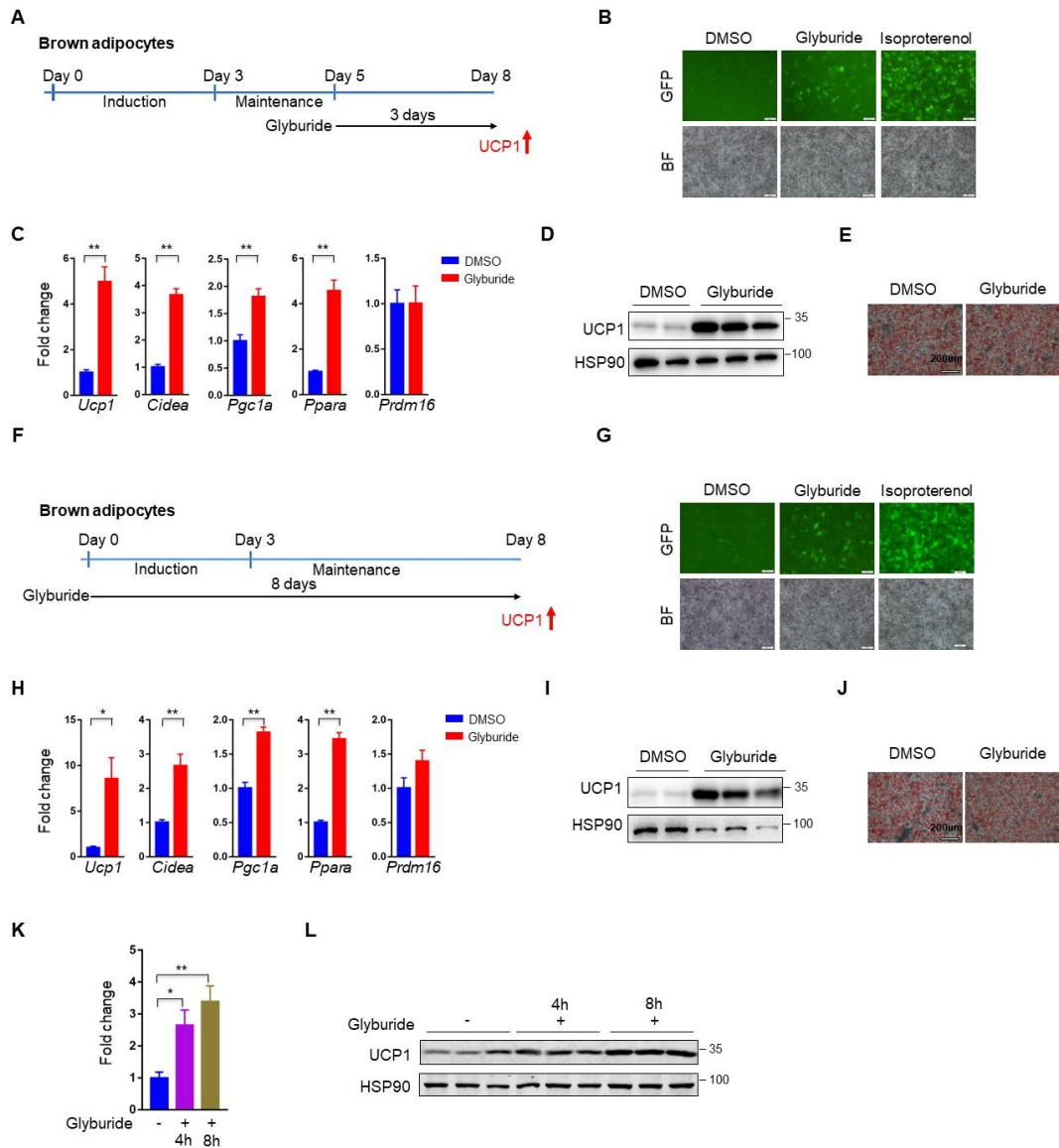


Figure S1. Glyburide promoted UCP1 expression in brown adipocytes *in vitro*, related to Figure 1. (A) Schematic view of the brown adipocyte differentiation procedure and compound treatment protocol. Cells were treated with 10 μ M glyburide for 3 days after 5 days' differentiation and collected at day 8 for analysis. (B) Representative images of GFP intensity of cells upon treatment with compounds at indicated. (C) mRNA expression analyses of genes in glyburide or DMSO-treated

Ucp1-2A-GFP brown adipocytes. n = 4. **(D)** Western blot analysis of UCP1 protein expression in glyburide or DMSO-treated *Ucp1-2A-GFP* brown adipocytes. **(E)** Assessment of lipid accumulation (evaluated by Oil Red-O staining) in glyburide or DMSO-treated *Ucp1-2A-GFP* brown adipocytes. **(F)** Schematic view of the brown adipocyte differentiation procedure and compound treatment protocol. Cells were treated with 10 μ M glyburide during the whole differentiation procedure and collected at day 8 for analysis. **(G)** Representative images of GFP intensity of cells upon treatment with compounds at indicated. **(H)** mRNA expression analyses of genes in glyburide or DMSO-treated *Ucp1-2A-GFP* brown adipocytes. n = 4. **(I)** Western blot analysis of UCP1 protein expression in glyburide or DMSO-treated *Ucp1-2A-GFP* brown adipocytes. **(J)** Assessment of lipid accumulation (evaluated by Oil Red-O staining) in glyburide or DMSO-treated *Ucp1-2A-GFP* brown adipocytes. **(K)** *Ucp1* mRNA expression analyses in glyburide or DMSO-treated brown adipocytes at indicated time points. n = 3. **(L)** UCP1 protein expression analyses in glyburide or DMSO-treated brown adipocytes at indicated time points. Scale bar = 200 μ m. Bars show mean \pm SEM. P values are shown for indicated comparisons by the Student's t test. * P < 0.05, ** P < 0.01.

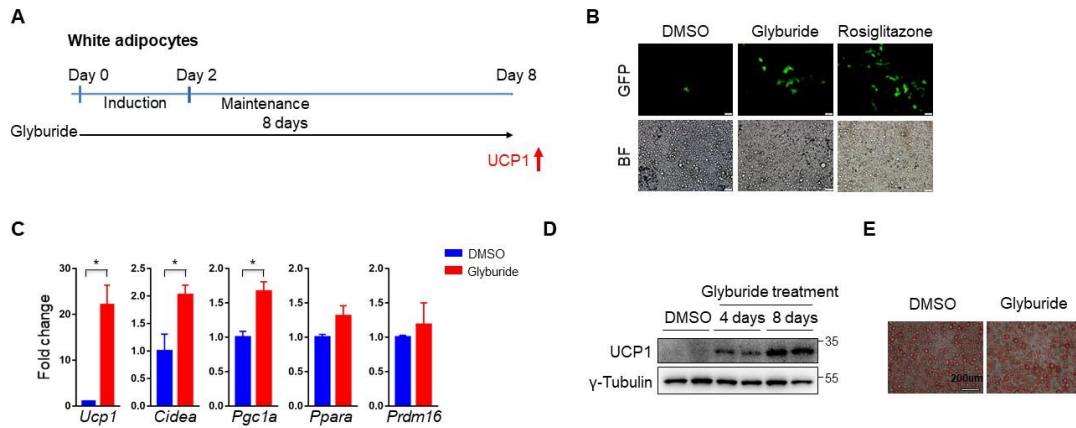


Figure S2. Glyburide promoted UCP1 expression in white adipocytes *in vitro*, related to Figure 1. (A) Schematic view of the white adipocyte differentiation procedure and compound treatment protocol. Cells were treated with 10 μ M glyburide during the whole differentiation procedure and collected at day 8 for analysis. (B) Representative images of GFP intensity of cells upon treatment with compounds at indicated. Scale bar = 50 μ m. (C) mRNA expression analyses of genes in glyburide or DMSO-treated *Ucp1-2A-GFP* white adipocytes. $n = 3$. (D) Western blot analysis of UCP1 protein expression in *Ucp1-2A-GFP* white adipocytes treated with glyburide for different days in comparison to DMSO-treated cells. (E) Assessment of lipid accumulation (evaluated by Oil Red-O staining) in glyburide or DMSO-treated *Ucp1-2A-GFP* white adipocytes. Scale bar = 200 μ m. Bars show mean \pm SEM. P values are shown for indicated comparisons by the Student's t test. * $P < 0.05$.

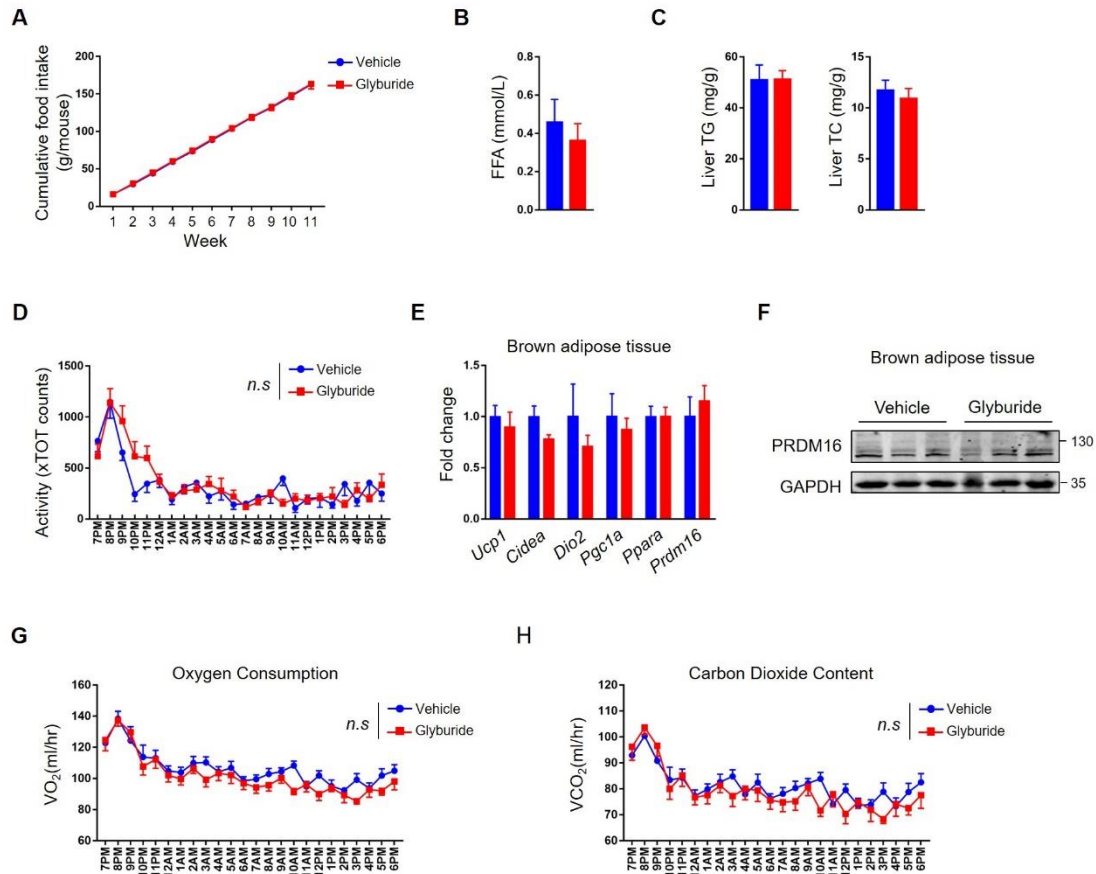


Figure S3. Glyburide treatment did not change food intake, physical activity or liver lipids levels in animals, related to Figure 2. (A) Accumulative food intake per mouse treated with 2 mg/kg/day glyburide or vehicle measured over 11-week. $n = 12$. **(B)** Free fatty acid (FFA) content of mice measured after 11-week treatment with 2 mg/kg glyburide or vehicle. $n = 6$. **(C)** Measurement of mouse liver TG and TC content in mice after 11-week treatment with 2 mg/kg/day glyburide or vehicle. $n = 6$. **(D)** Physical activity measurement of mice in metabolic cages after 11-week treatment with 2 mg/kg/day glyburide or vehicle. $n = 8$. **(E)** mRNA expression analyses of genes in brown adipose tissue of 2 mg/kg glyburide or vehicle-treated mice. $n = 6$. **(F)** Western blot analysis of PRDM16 protein expression level in brown adipose tissue of 2 mg/kg glyburide or vehicle-treated mice. **(G)** Oxygen consumption measurement of mice in metabolic cages after 11-week treatment with glyburide or vehicle. $n = 8$. **(H)** CO₂ content measurement of mice in metabolic cages after 11-week treatment with glyburide or vehicle. $n = 8$. Bars show mean \pm SEM. Student's *t* test (A-C, E) or two-way ANOVA (D, G and H). n.s = not significant.

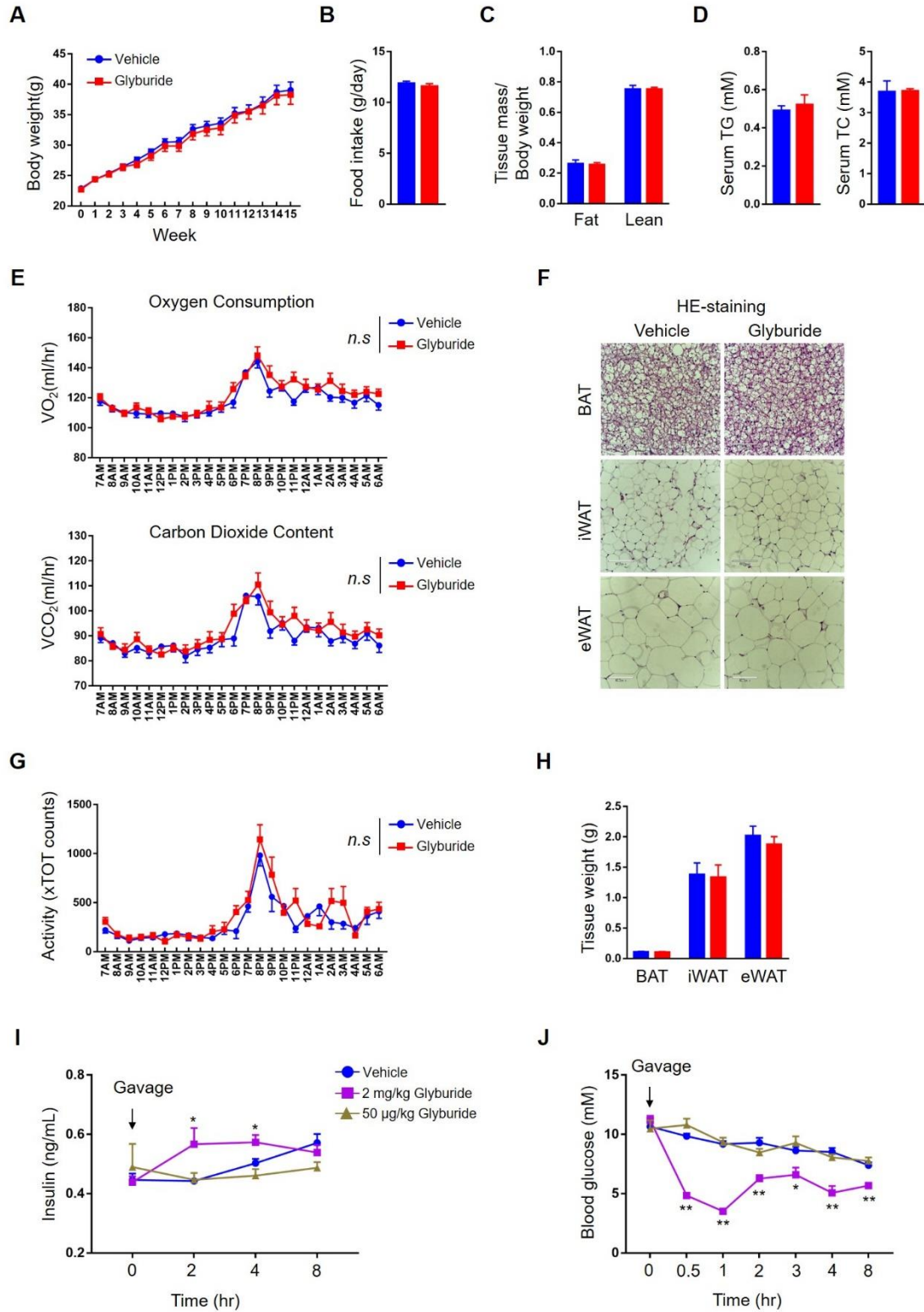


Figure S4. Physiological effects of animals after treatment with low dose of glyburide, related to Figure 2. (A) Body weights of mice treated with 50 µg/kg/day glyburide or vehicle under HFD. n = 10. **(B)** Food intake per mouse treated with 50 µg/kg/day glyburide or vehicle measured over 15-week. n = 10. **(C)** Body lean and fat

composition of mice determined by NMR after 8-week treatment with glyburide or vehicle. n = 12. **(D)** Serum total triglyceride (TG) and total cholesterol (TC) content of mice measured after 11-week treatment with glyburide or vehicle. n = 10. **(E)** Oxygen consumption and CO₂ content measurement of mice in metabolic cages after 14-week treatment with glyburide or vehicle. n = 8. **(F)** Representative HE staining images of BAT, iWAT, and eWAT. Scale bar = 210 μm. **(G)** Physical activity measurement of mice in metabolic cages after 14-week treatment with glyburide or vehicle. n = 8. **(H)** Weights of different mouse adipose tissues after 15-week treatment with glyburide or vehicle. n = 10. **(I)** Insulin response of mice treated with different doses of glyburide via oral administration. n = 7. **(J)** Blood glucose response of mice treated with different doses of glyburide via oral administration. n = 7. Bars show mean ± SEM. P values are shown for indicated comparisons by the Student's t test (A-D, H-J) or two-way ANOVA (E and G). * P < 0.05, ** P < 0.01. n.s = not significant.

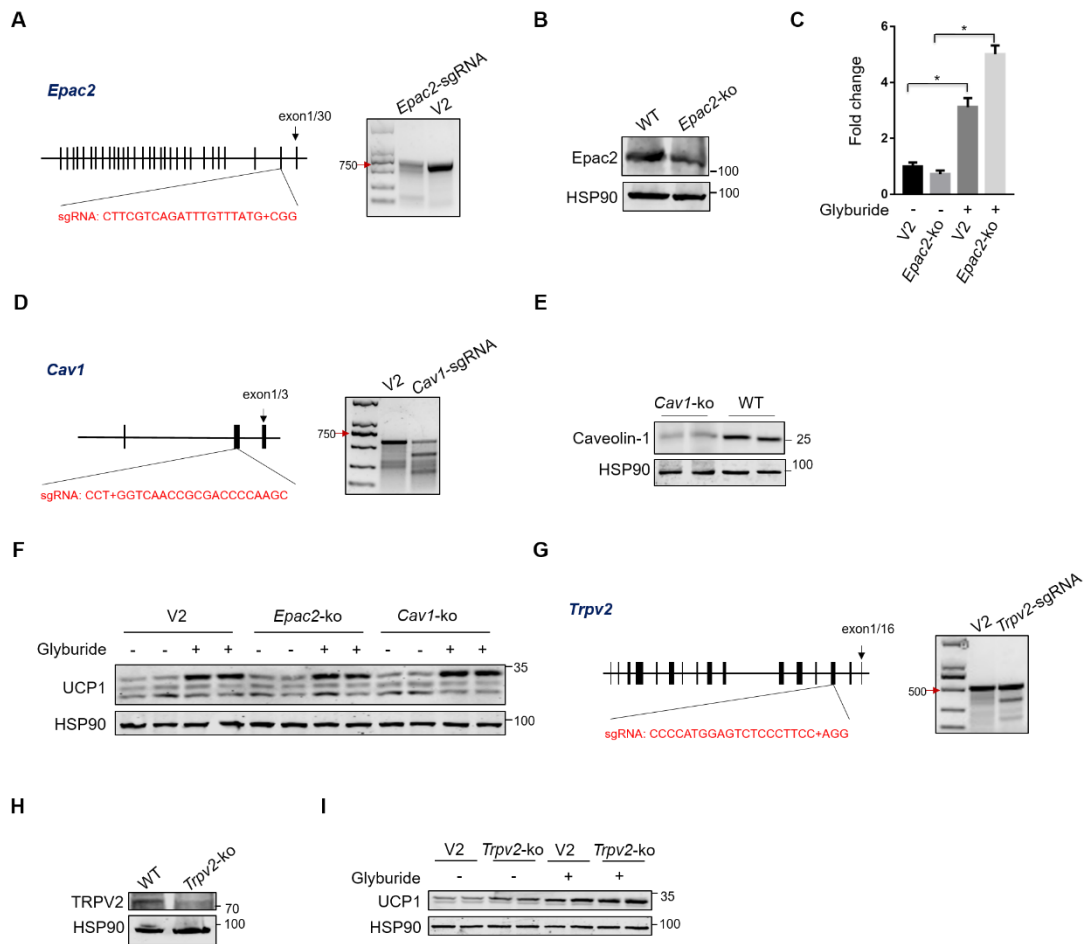


Figure S5. The glyburide's effect in UCP1 upregulation was not dependent on *Epac2*, *Cav1*, or *Trpv2*, related to Figure 4. (A) Schematic view of CRISPR sgRNA design for *Epac2* gene and genome editing activity of selected sgRNA as indicated. (B) *Epac2* protein expression analyses in cultured *Epac2*-KO versus control brown adipocytes. (C) *Ucp1* mRNA expression analyses of brown adipocytes treated with CRISPRs and compounds as indicated. n = 3. (D) Schematic view of CRISPR sgRNA design for *Cav1* gene and genome editing activity of selected sgRNA as indicated. (E) Caveolin 1 protein expression analyses in cultured *Cav1*-KO versus control brown adipocytes. (F) UCP1 protein expression analyses of brown adipocytes treated with CRISPRs and compounds as indicated. (G) Schematic view of CRISPR sgRNA design for *Trpv2* gene and genome editing activity of selected sgRNA as indicated. (H) TRPV2 protein expression analyses in cultured *Trpv2*-KO versus control brown adipocytes. (I) UCP1 protein expression analyses of brown adipocytes treated with CRISPRs and compounds as indicated. Bars show mean \pm SEM. P values are shown for indicated

comparisons by the Student's t test. * $P < 0.05$.

Gene Name	sgRNA Sequence	Primers Used in T7E1 Analysis
<i>Kir6.1</i>	CGAAGAGCAGCCAGCTGCAG	GTGCTAACTTCAACCCTGCAC
		TAGTCTAGGAGGACGCGTGT G
<i>Kir6.2</i>	GAAGATGCAGCCCAGCATGA	TCGTCAGCTAGGTAGGAGGT
		TCCACTCCTTTTCATCTGCCT
<i>Sur1</i>	CAGGACAAAGAGCAGCATGA	CAAAGATGAGGGCCCAGAGA
		TCATATGCTCATCCCTGGGG
<i>Sur2</i>	CAAACGTCAGAATCCATCTC	AAAGCAAGCCCCCATGGTTAT
		TGTCCCACTTTGTACCACCA
<i>Cav1</i>	GCTTGGGGTCGCGGTTGACC	GACTTCGCCCTGACCCCT
		AGGAAGAGGCAGGCAGATG
<i>Epac2</i>	CTTCGTCAGATTTGTTTATG	GCAGACCTTCCCTAGCTGTT
		TGTGGATGCTATCTGTCCCC
<i>Trpv2</i>	CCCCATGGAGTCTCCCTTCC	CTCCACAGAAGTTTCAGCGA
		CAAATGGGTGGGGTTCGAA

Table S1. The sequences of sgRNAs targeting different genes and the primers that used for T7E1 analysis, related to Figure 4 and Figure S5. The sequences of sgRNAs and primers for indicated genes were both from 5' to 3'.

Transparent Methods

Animals

C57BL/6J mice were fed with high fat diet (HFD, 60% of energy from fat, Research Diets, Inc., D12492) and treated with glyburide or vehicle by daily oral gavage. For low dose tests, animals were treated with glyburide (50 µg/kg/day) or vehicle (0.5% DMSO, H₂O) for 15 weeks; whereas in the high dose tests, animals were treated with glyburide (2 mg/kg/day) or vehicle (4.5% DMSO, 1% Tween, H₂O) for 11 weeks. The body weight and food intake were monitored weekly. Body fat content was determined by nuclear magnetic resonance (Echo MRI).

Adipocyte culture and differentiation

Brown pre-adipocytes and white pre-adipocytes were all maintained at 37 °C in 5% CO₂ in primary culture medium (high-glucose Dulbecco's modified Eagle's medium (DMEM) with 20% fetal bovine serum (FBS) and 1% penicillin/streptomycin). Adipocytes differentiation were performed following the protocols as described before (9, 10). Drugs used were as following: glyburide (10 µM, Selleck, S1716), Gliclazide (10 µM, Selleck, S2601), Nateglinide (10 µM, Selleck, S2489), Repaglinide (10 µM, Selleck, S1426), Tolbutamide (10 µM, Selleck, S2443), Diazoxide (10 µM, Selleck, S4630), Nitrendipine (30 µM, Selleck, S2491), Cyclosporine A (10 µM, MCE, HY-B0579), FK506 (10 µM, Selleck, S5003), VIVIT (10 µM, MCE, HY-P1026).

Oil Red-O staining in cultured brown and white adipocytes

Brown and white adipocytes were fixed in 4% paraformaldehyde for 20 min at room temperature, then incubated with 85% isopropanol for 1 min and incubated with preheated 60% oil red for 15 min.

CRISPR targeting

The 20 bp sequences of sgRNAs targeting different genes were inserted to lentiCRISPR-V2 plasmid (Addgene, 52961) and used for lentivirus packaging. Lentiviruses carrying CRISPR-Cas9 targeting different genes or empty lentiCRISPR-

V2 vector as control were packaged in HEK 293T cells. The brown or white pre-adipocytes were infected and selected with puromycin (1.5 µg/ml) to remove uninfected cells. Cells were next subjected to genomic DNA extraction for T7E1 analysis (NEB, E3321) to determine gene editing efficiency. The sequences of sgRNAs targeting different genes and the primers used for T7E1 analysis were list in Supplemental Table1.

***In situ* drug injection**

Eight weeks' old male C57BL/6J mice were injected bilaterally with 1 mg/kg glyburide, 1 mg/kg CL-316243 (Tocris, 1499) or solvent (0.5% DMSO, ddH₂O) as control into the inguinal fat pads after general anesthesia. The stock concentration of glyburide was 80 mg/ml dissolving in DMSO + PBS. CL-316243 was dissolved in ddH₂O. Mice were sacrificed after metabolic analysis, and inguinal fat pads were dissected for further analysis.

Blood glucose and plasma insulin measurements

Eight weeks' old male C57BL/6J mice were treated with 2 mg/kg glyburide, 50 µg/kg glyburide or vehicle by oral gavage. Blood glucose content was assayed with a glucometer (Abbott) after glyburide treatment at various times points as indicated. For plasma insulin measurements, blood was taken from the tail vein at indicated times (as indicated in figure), and measured using a rat insulin ELISA kit (ALPCO, 80-INSRTU-E01).

Cold challenge experiment

Eight weeks' old male C57BL/6J mice treated with glyburide or solvent control were individually caged without beddings and exposed to 4 °C for 6 hours. Rectal temperatures were measured each hour with a model BAT-12 thermometer (Physitemp Instruments).

Metabolic studies

Whole-body O₂ consumption, CO₂ production and physical activity were measured in metabolic cages (Columbus Instruments). Mice had access ad libitum to chow and

water in respiration chambers.

Lipid analysis in blood and liver tissues

For blood lipid analysis, animals were starved for 4 hours before tail-vein blood collection. Blood serum was further collected after centrifugation at 2,500 rpm for 20~30 min, and stored at -80 °C or used immediately for triglyceride or cholesterol measurement. All procedures were performed on ice.

For lipid analysis in liver tissues, lipids were extracted using a chloroform methanol (2:1) method. Briefly, liver tissues of around 30 mg were ground in 500 µl ice-cold PBS. Of which, 100 µl extracts were used for measurement for protein concentration, and the remaining 400 µl extracts were homogenized in 1.6 ml of a mixture of chloroform methanol (2:1). The suspension was then centrifuged at 2,500 rpm for 10 min at 4 °C, and the lower organic phase was transferred and air-dried in a chemical hood overnight. The residual liquid was later resuspended in 500 µl of absolute ethanol plus 1% Triton X-100 for subsequent triglyceride or cholesterol measurement.

Total triglyceride (TG) and total cholesterol (TC) in blood serum or extracted lipid samples from liver tissues were measured with TG and TC kit (Shanghai Shensuo UNF, 1030280, 1040280). TG and TC content measured in liver were further normalized to protein concentration.

RNA isolation and real-time quantitative PCR

Total RNA was extracted from cells or tissues using TRIzol reagent (ThermoFisher, 15596018) and transcribed with the reverse transcription kit (Takara, RR047A). Quantitative real-time PCR was carried out on the 7900 System (ABI) using SYBR Green supermix (ABI, 4472908). The sequences of primers were used as following: mouse *Ucp1* forward: 5'-GCATTCAGAGGCAAATCAGC-3' and reverse: 5'-GCCACACCTCCAGTCATTAAG-3'; mouse *Cidea* forward: 5'-GAATAGCCAGAGTCACCTTCG-3' and reverse: 5'-AGCAGATTCCTTAACACGGC-3'; mouse *Dio2* forward: 5'-GACTCGGTCATTCTGCTCAA-3' and reverse: 5'-

AGGCATCTAGGAGGAAGCTG-3'; mouse *Pgcla* forward: 5'-TCACGTTCAAGGTCACCCTA-3' and reverse: 5'-TCTCTCTCTGTTTGGCCCTT-3'; mouse *Ppara* forward: 5'-CATTTCCCTGTTTGTGGCTG-3' and reverse: 5'-ATCTGGATGGTTGCTCTGC-3'; mouse *Prdm16* forward: 5'-CCGACTTTGGATGGGAGATG-3' and reverse: 5'-CACGGATGTACTIONTGAGCCAG-3'; mouse *Actin* forward: 5'-GGTGGGAATGGGTCAGAAG-3' and reverse: 5'-AGCTCATTGTAGAAGGTGTGG-3'.

Western analysis

Protein from cells or tissues was extracted by RIPA buffer (Millipore, 20188) and subjected to regular western procedure. The primary antibodies used in the experiments were antibodies to UCP1 (Abcam, ab10983, RRID: AB_2241462), HSP90 (CST, 4874S, RRID: AB_2121214), Actin (Abclonal, AC004, RRID: AB_2737399), γ -Tubulin (Sigma, T6557, RRID: AB_477584), OXPHOS cocktail (Abcam, ab110413, RRID: AB_2629281), PRDM16 (Abclonal, A11581, RRID: AB_2758611), Kir6.1 (Bioss, BS-6468R), Kir6.2 (Bioss, BS-2436R, RRID: AB_10855420), SUR1 (Abclonal, A8456), Epac2 (Proteintech, 67044-1-1g), Caveolin-1 (Santa cruz, sc-70516, RRID: AB_1120056), and TRPV2 (Abclonal, A12367).

Histology

Mouse tissues were fixed and embedded in paraffin (for HE staining) or frozen (for UCP1 staining). Sections were stained with hematoxylin and eosin or UCP1 antibody (1:100, Abcam, ab10983) according to standard protocols (Wuhan servicebio technology).

RNA-seq analysis

RNA-seq analysis was performed following standard procedures. Sequencing of total RNA from brown or white adipocytes treated with glyburide or DMSO was performed in Majorbio Company (Shanghai). For data analysis, differentially expressed genes were identified using $P \leq 0.05$ as cutoff. GO term annotations were performed with

online software (<http://geneontology.org/>).

Statistics

The unpaired, two-tailed Student's t test or two-way ANOVA was used for experiments with two groups' comparison. one-way ANOVA test and post-hoc Bonferronic multiple-comparison test was used for experiments that contained more than two groups. All data are represented as means with SEM. * $P < 0.05$, ** $P < 0.01$. n.s = not significant.

Study approval

All mice were housed under standard conditions at the Shanghai Institutes for Biological Sciences (SIBS), China. All animal procedures were performed according to guidelines, and were approved by the Institutional Animal Care and Use Committee of the Shanghai Institutes for Biological Sciences.